Preliminary Communication

Raquib Alam, Md. Aftab Alam, Amulya K. Panda and Rahis Uddin*

Design, synthesis and cytotoxicity evaluation of novel (*E*)-3-(3-aryl-1-phenyl-1*H*-pyrazol-4-yl)-1-(pyridin-3-yl)prop-2-en-1-ones as anticancer agents

DOI 10.1515/hc-2016-0042
Received March 16, 2016; accepted June 1, 2016; previously published online July 18, 2016

Abstract: (*E*)-3-(3-Aryl-1-phenyl-1*H*-pyrazol-4-yl)-1-(pyridin-3-yl)prop-2-en-1-ones **4a–i** have been synthesized and evaluated for their *in vitro* cytotoxicity against a panel of three human cancer cell lines Caco-2, MIA PaCa-2, MCF-7 and a normal NIH-3T3 cell line. Compound **4g** is cytotoxic with the IC_{50} value of 15.32±0.62 μM against the Caco-2 cell line.

Keywords: chalcones; Claisen-Schmidt condensation; cytotoxic activity; pyrazoles.

Although there has been considerable progress in reducing cancer incidence in the United States, the number of cancer patients continues to increase [1]. Chemotherapy is one of the most effective approaches used for treating cancer patients. However, the lack of selectivity and development of drug-resistance reduces the efficacy of cancer chemotherapy [2]. Therefore development of effective and safe anticancer agents with high potency and less toxicity is a major focus for researchers across the world. The heterocyclic compounds containing a pyrazole ring have received considerable attention owing to their diverse chemotherapeutic potential [3–5]. Important pyrazole-based antitumor drugs available in the market include ruxolitinib and crizotinib [6]. Celecoxib is a typical model of pyrazole-based diaryl heterocyclic small molecule [7] with antitumor activity against prostate tumors in experimental models [8–10]. Chalcones show anti-cancer activity [11–28] apparently due to their inhibition of tubulin [15], thioredoxin reductase [17], VEGF [18], mTOR [19] topoisomerase-I/II [20], 5α-reductase [21], sirtuin-1 [22], JAK/STAT signaling pathways [23], MMP-2 [24], cathepsin-K [25], Wnt [26], B-Raf [27] and NF-κB [28], among others.

On the basis of the interesting biological activity profiles of pyrazoles and chalcones, we were inspired to synthesize some pyrazolic chalcones as potential anticancer agents. Synthesis is outlined in Scheme 1. Pyrazolic chalcones were prepared from the corresponding 3-aryl-1-phenylpyrazol-4-carboxaldehydes **3a–i** [29–33] which, in turn, were synthesized from the heterocyclic substrates **2a–i** [30] (see Supplementary Material). The Claisen-Schmidt condensation of compounds **3a–i** with 3-acetylpyridine in methanolic NaOH afforded the desired (*E*)-3-(3-(aryl)-1-phenyl-1*H*-pyrazol-4-yl)-pyridin-3-yl)prop-2-en-1-ones **4a–i**. Compounds **3a–i** and **4a–i** were characterized by spectral methods and elemental analysis.

In vitro cytotoxicity of compounds **4a–i** was measured by an MTT [(3-(4,5-dimethyl-2-thiazolyl)-2,5-diphenyl-2*H*-tetrazolium bromide)] assay against a panel of three

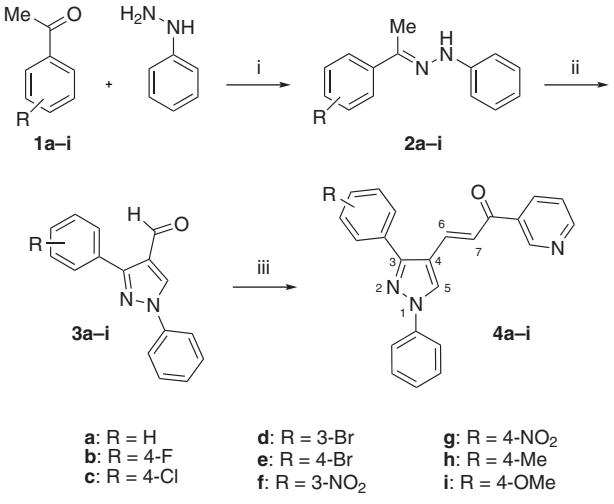

Scheme 1 Conditions: (i) EtOH, H_2SO_4, reflux; (ii) $POCl_3$/DMF, 80°C, then $NaHCO_3/H_2O$; (iii) 3-acetylpyridine, MeOH, NaOH, r.t.

***Corresponding author: Rahis Uddin,** Department of Chemistry, Jamia Millia Islamia (A Central University), Jamia Nagar, New Delhi 110025, India, e-mail: rahisuddin@jmi.ac.in
Raquib Alam: Department of Chemistry, Jamia Millia Islamia (A Central University), Jamia Nagar, New Delhi 110025, India
Md. Aftab Alam: Department of pharmacy, School of Medical and Allied Science, Galgotias University, Greater Noida 201301, UP, India
Amulya K. Panda: Product Development Cell, National Institute of Immunology, New Delhi 110067, India

Table 1 *In vitro* cytotoxicity evaluation of the synthesized compounds against a panel of human cancer cell lines and a normal cell line in terms of IC_{50} value in μM.

Compounds	R	Caco-2	MIA PaCa-2	MCF-7	NIH-3T3
4a	H	32.30±0.65	38.52±2.31	56.65±2.75	>100
4b	4-F	23.09±0.93	28.28±2.17	34.38±3.83	91.46±2.99
4c	4-Cl	38.93±2.49	46.57±2.30	54.53±1.10	92.58±2.52
4d	3-Br	30.28±2.01	24.80±1.46	46.67±2.01	96.56±1.55
4e	4-Br	27.95±0.29	30.40±0.84	39.79±1.07	96.13±2.09
4f	3-NO_2	19.62±0.76	19.70±0.32	29.78±0.84	87.58±1.96
4g	4-NO_2	15.32±0.62	18.89±0.44	29.59±2.18	87.39±0.44
4h	4-CH_3	37.83±2.85	21.94±5.10	68.78±1.16	>100
4i	4-OCH_3	49.12±8.37	32.05±1.23	44.36±1.08	>100
Etoposide	–	17.51±0.24	23.66±0.33	32.31±1.48	90.53±4.6

different human cancer cell lines, namely Caco-2 (human intestinal), MIA PaCa-2 (human pancreatic) and MCF-7 (human breast) and one normal cell line (mouse embryo fibroblasts NIH-3T3) [34]. Etoposide was taken as the reference drug and the results are summarized in terms of IC_{50} values (Table 1). Most of the compounds show moderate to good cytotoxicity against intestinal, pancreatic and breast cancer cell lines and very weak toxicity towards NIH-3T3 normal cell line. Analogs **4f–h** show significant cytotoxicity as compared to standard drug etoposide. Out of 9 pyrazolic chalcones synthesized, compound **4g** displays the most potent cytotoxicity against Caco-2 cell line. SAR analysis of these pyrazolic chalcones indicate that compounds with a *para* substituted NO_2 group in the benzene ring are more cytotoxic. Compounds with F, Cl, Br, CH_3 or OCH_3 substituent show more moderate effects, which is clearly seen from Table 1. The cytotoxic activity against all tested cancer cell lines shows that the strength order is NO_2>F>Br>Cl for compounds with a *para* substituted electron-withdrawing group present in the benzene ring. Among compounds with *meta* substituted electron-withdrawing group, the cytotoxic activity order is NO_2>Br. Finally, cytotoxic activity against Caco-2 and MIA PaCa-2 shows that the strength order is CH_3>OCH_3 for compounds with electron-donating substituent present in *para* position of the benzene ring. Furthermore, cytotoxic activity against MCF-7 shows the strength order is OCH_3>CH_3 for compounds with *para* electron-donating substituent.

Experimental

All starting materials and solvents were purchased from commercial sources and used without further purification. Melting points were determined in open capillaries using an electro-thermal melting point apparatus and are uncorrected. The progress of the reactions was monitored by TLC using precoated aluminum sheets (Silica gel 60 F_{254}, Merck) and spots were visualized under UV light. IR spectra were recorded on an Agilent Cary 630 FT-IR spectrometer. The ^{1}H NMR (400 MHz) and ^{13}C NMR (100 MHz) spectra were recorded on a Bruker Avance 400 spectrometer using $CDCl_3$ or DMSO-d_6 as a solvent and TMS as an internal standard. Elemental analysis were performed on an Elementar Vario analyzer. Mass spectra (ESI-MS) were recorded on an AB-Sciex 2000 spectrometer.

General synthesis of compounds 4a–i

A mixture of 3-aryl-1-phenylpyrazol-4-carboxaldehyde **3a–i** (10 mmol) and 3-acetylpyridine (10 mmol) in methanolic solution of sodium hydroxide was stirred for 24 h at room temperature. The resultant precipitate of **4a–i** was filtered off, washed with water, dried, and crystallized from ethanol (**4a–e** and **4h,i**) or *N,N*-dimethylformamide (**4f,g**).

(E)-3-(1,3-Diphenyl-1*H*-pyrazol-4-yl)-1-(pyridin-3-yl)prop-2-en-1-one (4a) Yellow solid; yield 64%; mp 168–170°C; IR (neat, ν_{max}): 3132, 1665, 1585, 1415 cm^{-1}; ^{1}H NMR ($CDCl_3$): δ 9.13 (s, 1H), 8.73–8.75 (m, 1H), 8.37(s, 1H), 8.21 (m, 1H), 7.91 (d, *J* = 15.6 Hz, 1H), 7.26–7.78 (m, 12H); ^{13}C NMR ($CDCl_3$): δ 188.5, 154.0, 153.0, 149.6, 139.3, 136.5, 135.7, 133.5, 132.1, 129.6, 128.9, 128.8, 128.8, 127.3, 127.2, 123.6, 120.5, 119.3, 117.9. ESI-MS. Calcd for $C_{23}H_{17}N_3O$, $[M + H]^+$: *m/z* 352.1. Found: *m/z* 352.2. Anal. Calcd for $C_{23}H_{17}N_3O$: C, 78.61; H, 4.55; N, 11.96. Found: C, 78.33; H, 4.84; N, 11.94.

(*E*)-3-(3-(4-Fluorophenyl)-1-phenyl-1*H*-pyrazol-4-yl)-1-(pyridin-3-yl)prop-2-en-1-one (4b) Yellow solid; yield: 70%; mp 170–172°C; IR (neat, ν_{max}): 3119, 1667, 1596, 1525, 1419 cm^{-1}; ^{1}H NMR ($CDCl_3$): δ 9.20 (s, 1H), 8.80 (d, *J* = 3.6 Hz, 1H), 8.40 (s, 1H), 8.28 (d, *J* = 8 Hz, 1H), 7.91 (d, *J* = 15.6 Hz, 1H), 7.80 (d, *J* = 8 Hz, 2H), 7.33–7.70 (m, 7H), 7.20 (t, *J* = 8.4 Hz, 2H); ^{13}C NMR ($CDCl_3$): δ 188.4, 164.4, 162.0, 153.1, 149.6, 139.2, 136.2, 135.8, 133.4, 130.6, 130.5, 129.6, 128.2, 127.5, 127.1, 123.7, 120.6, 119.4, 117.9, 116.0, 115.8. ESI-MS. Calcd for $C_{23}H_{16}FN_3O$, $[M + H]^+$: *m/z* 370.1. Found: *m/z* 370.5. Anal. Calcd for $C_{23}H_{16}FN_3O$: 74.78; H, 4.37; N, 11.38. Found: C, 74.73; H, 4.39; N, 11.41.

(*E*)-3-(3-(4-Chlorophenyl)-1-phenyl-1*H*-pyrazol-4-yl)-1-(pyridin-3-yl)prop-2-en-1-one (4c) Yellow solid; yield 64%; mp 162–164°C; IR (neat, ν_{max}): 3134, 1665, 1583, 1501, 1404 cm^{-1}; ^{1}H NMR ($CDCl_3$): δ 9.16 (s, 1H), 8.76 (d, *J* = 4.4 Hz, 1H), 8.37 (s, 1H), 8.21 (d, *J* = 8 Hz, 1H), 7.85 (d, *J* = 15.2 Hz, 1H), 7.76 (d, *J* = 8 Hz, 2H), 7.61 (d, *J* = 8.4 Hz, 2H),

7.29–7.50 (m, 7H); ^{13}C NMR ($CDCl_3$): δ 188.8, 153.1, 152.8, 149.6, 139.2, 136.0, 135.7, 134.9, 133.4, 130.6, 130.0, 129.6, 129.0, 127.5, 127.1, 123.7, 120.8, 119.4, 117.9. ESI-MS. Calcd for $C_{23}H_{16}ClN_3O$, $[M + H]^+$: *m/z* 386.1. Found: *m/z* 386.4. Anal. Calcd for $C_{23}H_{16}ClN_3O$: C, 71.59; H, 4.18; N, 10.89. Found: C, 71.65; H, 4.16; N, 10.85.

(*E*)-3-(3-(3-Bromophenyl)-1-phenyl-1*H*-pyrazol-4-yl)-1-(pyridin-3-yl)prop-2-en-1-one (4d) Yellow solid; yield 82%; mp 172–174°C; IR (neat, ν_{max}): 3136, 1663, 1596, 1493, 1404 cm^{-1}; ^{1}H NMR ($CDCl_3$): δ 9.17 (s, 1H), 8.80 (d, *J* = 3.2 Hz, 1H), 8.39 (s, 1H), 8.26 (d, *J* = 7.6 Hz, 1H), 7.89 (d, *J* = 15.2 Hz, 2H), 7.80 (d, *J* = 8 Hz, 2H), 7.36–7.62 (m, 8H); ^{13}C NMR ($CDCl_3$): δ 188.5, 153.1, 152.3, 149.6, 139.1, 135.8, 135.8, 134.2, 133.4, 131.8, 131.6, 130.3, 129.6, 127.6, 127.4, 127.3, 123.6, 122.9, 121.0, 119.4, 118.0. ESI-MS. Calcd. for $C_{23}H_{16}BrN_3O$, $[M + H]^+$: *m/z* 430.05. Found: *m/z* 430.04. Anal. Calcd for $C_{23}H_{16}BrN_3O$: C, 64.20; H, 3.75; N, 9.77. Found: C, 64.26; H, 3.71; N, 9.75.

(*E*)-3-(3-(4-Bromophenyl)-1-phenyl-1*H*-pyrazol-4-yl)-1-(pyridin-3-yl)prop-2-en-1-one (4e) Yellow solid; yield 75%; mp 158–160°C; IR (neat, ν_{max}): 3136, 1663, 1596, 1501, 1400 cm^{-1}; ^{1}H NMR ($CDCl_3$): δ 9.20 (s, 1H), 8.80 (d, *J* = 4.4 Hz, 1H), 8.40 (s, 1H), 8.27 (d, *J* = 7.6 Hz, 1H), 7.90 (d, *J* = 15.6 Hz, 1H), 7.80 (d, *J* = 8 Hz, 2H), 7.64 (d, *J* = 8 Hz, 2H), 7.58 (d, *J* = 8 Hz, 2H), 7.33–7.53 (m, 5H); ^{13}C NMR ($CDCl_3$): δ 188.3, 153.1, 152.8, 149.6, 139.1, 136.0, 135.8, 133.4, 132.0, 131.0, 130.2, 129.6, 127.5, 127.1, 123.7, 123.2, 120.8, 119.3, 117.9. ESI-MS. Calcd for $C_{23}H_{16}BrN_3O$, $[M + H]^+$: *m/z* 430.05. Found: 430.04. Anal. Calcd for $C_{23}H_{16}BrN_3O$: C, 64.20; H, 3.75; N, 9.75. Found: C, 64.14; H, 3.77; N, 9.79.

(*E*)-3-(3-(3-Nitrophenyl)-1-phenyl-1*H*-pyrazol-4-yl)-1-(pyridin-3-yl)prop-2-en-1-one (4f) Yellow solid; yield 69%; mp 206–208°C; IR (neat, ν_{max}): 3136, 1665, 1596, 1533, 1423, 1344 cm^{-1}; ^{1}H NMR (DMSO-d_6): δ 9.40 (s, 1H), 9.24 (d, *J* = 1.6 Hz, 1H), 8.78–8.80 (m, 1H), 8.40 (s, 1H), 8.32 (d, *J* = 8 Hz, 1H), 8.27 (d, *J* = 8 Hz, 1H), 8.06 (d, *J* = 8 Hz, 1H), 7.77–7.89 (m, 4H), 7.65 (d, *J* = 15.2 Hz, 1H), 7.37–7.58 (m, 4H); ^{13}C NMR (DMSO-d_6): δ 188.1, 153.7, 150.8, 149.9, 148.5, 139.1, 136.0, 134.9, 134.3, 133.8, 133.1, 131.0, 130.1, 129.9, 127.9, 124.4, 123.8, 122.9, 122.2, 119.2, 118.4. ESI-MS. Calcd. for $C_{23}H_{16}N_4O_3$, $[M + H]^+$: *m/z* 397.2. Found: *m/z* 397.2. Anal. Calcd for $C_{23}H_{16}N_4O_3$: C, 69.69; H, 4.07; N, 14.13. Found: C, 69.65; H, 4.08; N, 14.16.

(*E*)-3-(3-(4-Nitrophenyl)-1-phenyl-1*H*-pyrazol-4-yl)-1-(pyridin-3-yl)prop-2-en-1-one (4g) Yellow solid; yield 76%; mp 220–222°C; IR (neat, ν_{max}): 3131, 1669, 1596, 1542, 1512, 1421, 1346 cm^{-1}; ^{1}H NMR (DMSO-d_6): δ 9.38 (s, 1H), 9.23 (s, 1H), 8.78 (d, *J* = 3.6 Hz, 1H), 7.80–8.32 (m, 8H), 7.63 (d, *J* = 15.2 Hz, 1H), 7.34–7.57 (m, 4H, 1H); ^{13}C NMR (DMSO-d_6): δ 187.9, 153.7, 150.8, 149.9, 147.6, 139.0, 138.6, 136.0, 134.3, 133.1, 130.1, 129.9, 129.6, 127.9, 124.4, 124.4, 122.2, 119.2, 118.7. ESI-MS. Calcd for $C_{23}H_{16}N_4O_3$, $[M + H]^+$: *m/z* 397.2. Found: *m/z* 397.2. Anal. Calcd for $C_{23}H_{16}N_4O_3$: C, 69.69; H, 4.07; N, 14.13. Found: C, 69.67; H, 4.08; N, 14.14.

(*E*)-3-(1-Phenyl-3-p-tolyl-1*H*-pyrazol-4-yl)-1-(pyridin-3-yl)prop-2-en-1-one (4h) Yellow Solid; yield 61%; mp 146–148°C; IR (neat, ν_{max}): 3119, 1667, 1596, 1538, 1499, 1419 cm^{-1}; ^{1}H NMR ($CDCl_3$): δ 9.15 (s, 1H), 8.76 (d, *J* = 3.2 Hz, 1H), 8.36 (s, 1H), 8.21 (d, *J* = 8Hz, 1H), 7.91 (d, *J* = 15.6 Hz, 1H), 7.77 (d, *J* = 7.6 Hz, 2H), 7.57 (d, *J* = 8Hz, 2H), 7.26–7.49 (m, 7H), 2.41 (s, 3H); ^{13}C NMR ($CDCl_3$): δ 188.5, 154.1, 152.9, 149.6, 139.3, 138.8, 136.7, 135.8, 133.6, 129.5, 129.5, 129.2, 128.6, 127.3, 127.1, 123.6, 120.4, 119.3, 117.9, 21.3. ESI-MS. Calcd for $C_{24}H_{19}N_3O$, $[M + H]^+$: *m/z* 366.1. Found: *m/z* 366.2. Anal. Calcd for $C_{24}H_{19}N_3O$: C, 78.88; H, 5.24; N, 11.50. Found: C, 78.85; H, 5.25; N, 11.52.

(*E*)-3-(3-(4-Methoxyphenyl)-1-phenyl-1*H*-pyrazol-4-yl)-1-(pyridin-3-yl)prop-2-en-1-one (4i) Yellow solid; yield 61%; mp 158–160°C; IR (neat, ν_{max}): 3119, 1665, 1596, 1525, 1503, 1419 cm^{-1}; ^{1}H NMR ($CDCl_3$): δ 9.15 (s, 1H), 8.74 (d, *J* = 4.8 Hz, 1H), 8.35 (s, 1H), 8.21 (d, *J* = 8Hz, 1H), 7.89 (d, *J* = 15.6 Hz, 1H), 7.76 (d, *J* = 8 Hz, 2H), 7.60 (d, *J* = 8.4 Hz, 2H), 7.26–7.47 (m, 5H), 6.99 (d, *J* = 8.8 Hz, 2H), 3.83 (s, 3H); ^{13}C NMR ($CDCl_3$): δ 188.5, 160.2, 153.9, 153.0, 149.6, 139.3, 136.7, 135.7, 133.5, 130.0, 129.5, 127.2, 127.0, 124.5, 123.6, 120.2, 119.3, 117.8, 114.3, 55.3. ESI-MS. Calcd for $C_{24}H_{19}N_3O_2$, $[M + H]^+$: *m/z* 382.1. Found: *m/z* 382.2. Anal. Calcd for $C_{24}H_{19}N_3O_2$: C, 75.57; H, 5.02; N, 11.02. Found: C, 75.54; H, 5.03; N, 11.04.

In vitro cytotoxic activity

The MTT [(3-(4, 5-dimethyl-2-thiazolyl) 2,5-diphenyl-2H-tetrazolium bromide)] assay is based on conversion of yellow, water soluble tetrazolium dye to a water-insoluble purple formazan by living cells. The amount of formazan crystals generated is directly proportional to the number of viable cells. The Caco-2, MIA PaCa-2, MCF-7 and NIH-3T3 cells were grown (37°C, 5% CO_2 in water jacketed incubator shell) using DMEM media with 10% FBS (fotal bovine serum), seeded on a single 96 well plate and allowed to adhere for MTT assays. The plate was treated with increasing concentrations of 1, 12.5, 25, 50 and 100 μM of the compounds. These concentrations were used in triplicate to the single 96 well tissue culture plate. After 24 h of treatment, the MTT assay was performed to check cell viability. For the MTT assay, the media were removed from all the wells, 10 μL of MTT reagent per well from a working stock (5 mg/mL) was added and the plates were incubated (37°C and 5% CO_2) for 2–3 h, and then the reagent was removed and the crystals were dissolved in dimethyl sulfoxide. The absorbance was measured at a test wavelength of 570 nm using an ELISA plate reader, LMR-340 M with a microplate reader. The percentage inhibition was calculated by the formulae:

$$\% \text{ Inhibition} = 100 - \frac{\text{Mean OD of treated cells}}{\text{Mean OD of the vehicle control cells (negative control)}} \times 100$$

Each assay was repeated three times. The IC_{50} values were calculated from the dose effect curve (Figure S1) and expressed as concentration (μM) of drug [34].

Acknowledgments: The authors thank the Head, Department of Chemistry, JMI, New Delhi, for providing research facilities, Prof. Vibha Tandon and Dr. Mohammad Abid for helpful discussions, and UGC, New Delhi, for research fellowship for Raquib Alam.

References

[1] Siegel, R.; DeSantis, C.; Virgo, K.; Stein, K.; Mariotto, A.; Smith, T.; Cooper, D.; Gansler, T.; Lerro, C.; Fedewa, S.; et al. Cancer treatment and survivorship statistics. *CA Cancer J. Clin.* **2012**, *62*, 220–241.

[2] Wu, Q.; Yang, Z.; Nie, Y.; Shi, Y.; Fan, D. Multi-drug resistance in cancer chemotherapeutics: mechanisms and lab approaches. *Cancer Lett.* **2014**, *347*, 159–166.
[3] Fustero, S.; Sanchez-Rosello, M.; Barrio, P.; Simon-Fuentes, A. From 2000 to Mid-2010: a fruitful decade for the synthesis of pyrazoles. *Chem. Rev.* **2011**, *111*, 6984–7034.
[4] Raffa, D.; Maggio, B.; Raimondi, M. V.; Cascioferro, S.; Plescia, F.; Cancemi, G.; Daidone, G. Recent advanced in bioactive systems containing pyrazole fused with a five membered heterocycle. *Eur. J. Med. Chem.* **2015**, *97*, 732–746.
[5] Küçükgüzel, S. G.; Senkardes, S. Recent advances in bioactive pyrazoles. *Eur. J. Med. Chem.* **2015**, *97*, 786–815.
[6] Bronson, J.; Dhar, M.; Ewing, W.; Lonberg, N. Chapter thirty-one-to market, to market-2011. *Annu. Rep. Med. Chem.* **2012**, *47*, 499–569.
[7] Palomer, A.; Cabre, F.; Pascual, J.; Campos, J.; Trujillo, M. A.; Entrena, A.; Gallo, M. A.; Garcia, L.; Mauleon, D.; Espinosa, A. Identification of novel cyclooxygenase-2 selective inhibitors using pharmacophore models. *J. Med. Chem.* **2002**, *45*, 1402–1411.
[8] Hsu, A. L.; Ching, T. T.; Wang, D. S.; Song, X.; Rangnekar, V. M.; Chen, C. S. The cyclooxygenase-2 inhibitor celecoxib induces apoptosis by blocking Akt activation in human prostate cancer cells independently of Bcl-2. *J. Biol. Chem.* **2000**, *275*, 11397–11403.
[9] Williams, C. S.; Watson, A. J.; Sheng, H.; Helou, R.; Shao, J.; DuBois, R. N. Celecoxib prevents tumor growth *in vivo* without toxicity to normal gut: lack of correlation between *in vitro* and *in vivo* models. *Cancer Res.* **2000**, *60*, 6045–6051.
[10] Kulp, S. K.; Yang, Y. T.; Hung, C. C.; Chen, K. F.; Lai, J. P.; Tseng, P. H.; Fowble, J. W.; Ward, P. J.; Chen, C. S. 3-Phosphoinositide-dependent protein kinase-1/Akt signaling represents a major cyclooxygenase-2-independent target for celecoxib in prostate cancer cells. *Cancer Res.* **2004**, *64*, 1444–1451.
[11] Arasavelli, A. M.; Ganapavarapu, V.; Vidavalur, S. Design, synthesis, and anti-cancer activity of novel aryl/heteroaryl chalcone derivatives. *Heterocycl. Commun.* **2016**, *22*, 1–5.
[12] Lee, D. H.; Jung, Y. J.; Koh, D.; Lim, Y.; Lee, Y. H.; Shin, S. Y. A synthetic chalcone, 2′-hydroxy-2,3,5′-trimethoxychalcone triggers unfolded protein response-mediated apoptosis in breast cancer cells. *Cancer Lett.* **2016**, *372*, 1–9.
[13] Winter, E.; Neuenfeldt, P. D.; Chiaradia-Delatorre, L. D.; Gauthier, C.; Yunes, R. A.; Nunes, R. J.; Creczynski-Pasa, T. B.; Pietro, A. D. Symmetric bis-chalcones as a new type of breast cancer resistance protein inhibitors with a mechanism different from that of chromones. *J. Med. Chem.* **2014**, *57*, 2930–2941.
[14] Nelson, G.; Alam, M. A.; Atkinson, T.; Gurrapu, S.; Kumar, J. S.; Bicknese, C.; Williams, J. L. Synthesis and evaluation of *p-N*,*N*-dialkyl substituted chalcones as anti-cancer agents. *Med. Chem. Res.* **2013**, *22*, 4610–4614.
[15] Yang, Z.; Wu, W.; Wang, J.; Liu, L.; Li, L.; Yang, J.; Wang, G.; Cao, D.; Zhang, R.; Tang, M.; et al. Synthesis and biological evaluation of novel millepachine derivatives as a new class of tubulin polymerization inhibitors. *J. Med. Chem.* **2014**, *57*, 7977–7989.
[16] Insuasty, B.; Tigreros, A.; Orozco, F.; Quiroga, J.; Abonia, R.; Nogueras, M.; Sanchez, A.; Cobo, J. Synthesis of novel pyrazolic analogues of chalcones and their 3-aryl-4-(3-aryl-4,5-dihydro-1*H*-pyrazol-5-yl)-1-phenyl-1*H*-pyrazole derivatives as potential antitumor agents. *Bioorg. Med. Chem.* **2010**, *18*, 4965–4974.
[17] Zhang, B.; Duan, D.; Ge, C.; Yao, J.; Liu, Y.; Li, X.; Fang, J. Synthesis of xanthohumol analogues and discovery of potent thioredoxin reductase inhibitor as potential anticancer agent. *J. Med. Chem.* **2015**, *58*, 1795–1805.
[18] Wang, Z.; Wang. N.; Han, S.; Wang, D.; Mo. S.; Yu, L.; Huang, H.; Tsui, K.; Shen, J.; Chen, J. Dietary compound isoliquiritigenin inhibits breast cancer neoangiogenesis via VEGF/VEGFR-2 signaling pathway. *PLoS One* **2013**, *8*, e68566.
[19] Yo, Y.; Shieh, G.; Hsu, K.; Wu, C.; Shiau, A.; Licorice and Licochalcone-A induce autophagy in LNCaP prostate cancer cells by suppression of Bcl-2 expression and the mTOR pathway. *J. Agric. Food Chem.* **2009**, *57*, 8266–8273.
[20] Abdel-Aziz, M.; Park, S.; El-Din, G.; Abuo-Rahma, A. A.; Sayed, M. A.; Kwon, Y. Novel N-4-piperazinyl-ciprofloxacin-chalcone hybrids: synthesis, physicochemical properties, anticancer and topoisomerase I and II inhibitory activity. *Eur. J. Med. Chem.* **2013**, *69*, 427–438.
[21] Shimizu, K.; Kondo, R.; Sakai, K.; Buabarn, S.; Dilokkunanant, U. A geranylated chalcone with 5α-reductase inhibitory properties from *Artocarpus incises*. *Phytochem.* **2000**, *54*, 737–739.
[22] Kahyo, T.; Ichikawa, S.; Hatanaka, T.; Yamada, M. K.; Setou, M. A novel chalcone polyphenol inhibits the deacetylase activity of SIRT1 and cell growth in HEK293T cells. *J. Pharmacol. Sci.* **2008**, *108*, 364–371.
[23] Pinz, S.; Unser, S.; Brueggemann, S.; Besl, E.; Al-Rifai, N.; Petkes, H.; Amslinger, S.; Rascle, A. The synthetic α-bromo-20,3,4,4′-tetramethoxychalcone (α-Br-TMC) inhibits the JAK/STAT signaling pathway. *PLoS One* **2014**, *9*, e90275.
[24] Ngameni, B.; Touaibia, M.; Patnam, R.; Belkaid, A.; Sonna, P.; Ngadjui, B. T.; Annabi, B.; Roy, R. Inhibition of MMP-2 secretion from brain tumor cells suggests chemopreventive properties of a furanocoumarin glycoside and of chalcones isolated from the twigs of *Dorstenia turbinate*. *Phytochem.* **2006**, *67*, 2573–2579.
[25] Ramalho, S. D.; Bernades, A.; Demetrius, G.; Noda-Perez, C.; Vieira, P. C.; dos Santos, C. Y.; da Silva, J. A.; de Moraes, M. O.; Mousinho, K.C. Synthetic chalcone derivatives as inhibitors of cathepsins K and B, and their cytotoxic evaluation. *Chem. Biodivers*. **2013**, *10*, 1999–2006.
[26] Cho, M.; Ryu, M.; Jeong, Y.; Chung, Y. H.; Kim, D. E.; Cho, H. S.; Kang, S.; Han, J. S.; Chang, M. Y.; Lee, C. K.; et al. Cardamonin suppresses melanogenesis by inhibition of Wnt/beta-catenin signalling. *Biochem. Biophys. Res. Commun.* **2009**, *3*, 500–505.
[27] Li, Q.; Li, C.; Lu, X.; Zhang, H.; Zhu, H. Design, synthesis and biological evaluation of novel (E)-α-benzylsulfonyl chalcone derivatives as potential BRAF inhibitors. *Eur. J. Med. Chem.* **2012**, *50*, 288–295.
[28] Orlikova, B.; Schnekenburger, M.; Zloh, M.; Golais, F.; Diederich, M.; Tasdemir, D. Natural chalcones as dual inhibitors of HDACs and NF-κB. *Oncol. Reports* **2012**, *28*, 797–805.
[29] Kira, M. A.; Adbel-Raeman, M. O.; Gadalla, K. Z. The vilsmeier-haack reaction-III Cyclization of hydrazones to pyrazoles. *Tetrahedron Lett.* **1969**, *10*, 109–110.
[30] Yadlapalli, R. K.; Chourasia, O. P.; Vemuri, K.; Sritharan, M.; Perali, R. S. Synthesis and *in vitro* anticancer and antitubercular activity of diarylpyrazole ligated dihydropyrimidines possessing lipophilic carbamoyl group. *Bioorg. Med. Chem. Lett.* **2012**, *22*, 2708–2711.

[31] Desai, N. C.; Joshi, V. V.; Rajpara, K. M.; Vaghani, H. V.; Satodiya, H. M. Facile synthesis of novel fluorine containing pyrazole based thiazole derivatives and evaluation of antimicrobial activity. *J. Fluorine Chem.* **2012**, *142*, 67–78.

[32] Elkady, M.; Nieß, R.; Schaible, A. M.; Bauer, J.; Luderer, S.; Ambrosi, G.; Werz, O.; Laufer, S. A. Modified acidic nonsteroidal anti-inflammatory drugs as dual inhibitors of mPGES-1 and 5-LOX. *J. Med. Chem.* **2012**, *55*, 8958–8962.

[33] Prakash, O.; Pannu, K.; Kumar, A. Synthesis of some new 2-(3-aryl-1-phenyl-4-pyrazolyl)-benzoxazoles using hypervalent iodine mediated oxidative cyclization of Schiff's bases. *Molecules* **2006**, *11*, 43–48.

[34] Mosmann, T. Rapid colorimetric assay for cellular growth and survival: Application to proliferation and cytotoxicity assays. *J. Immunol. Methods* **1983**, *65*, 55–63.

Supplemental Material: The online version of this article (DOI: 10.1515/hc-2016-0042) offers supplementary material, available to authorized users.